Optical protection of a collective state from inhomogeneous dephasing

R. Finkelstein, O. Lahad, I. Cohen, O. Davidson, S. Kiriati, E. Poem, and O. Firstenberg Physics of Complex Systems, Weizmann Institute of Science, Rehovot 7610001, Israel Department of Physics and Astronomy, Arhus University, Ny Munkegade 120, DK-8000 Arhus C, Denmark

We introduce and demonstrate a scheme for eliminating the inhomogeneous dephasing of a collective quantum state. The scheme employs off-resonant optical fields that dress the collective state with an auxiliary sensor state, which has an enhanced and opposite sensitivity to the same source of inhomogeneity. We derive the optimal conditions under which the dressed state is fully protected from dephasing, when using either one or two dressing fields. The latter provides better protection, prevents global phase rotation, and suppresses the sensitivity to drive noise. We further provide expressions for all residual, higher-order, sensitivities. We experimentally study the scheme by protecting a collective excitation of an atomic ensemble, where inhomogeneous dephasing originates from thermal motion. Using photon storage and retrieval, we demonstrate complete suppression of inhomogeneous dephasing and consequently a prolonged memory time. Our scheme may be applied to eliminate motional dephasing in other systems, improving the performance of quantum gates and memories with neutral atoms. It is also generally applicable to various gas, solid, and engineered systems, where sensitivity to variations in time, space, or other domains limits possible scale-up of the system.

The quantum state of a system is prone to decoherence via inhomogeneous dephasing due to variations among the system's constituents. These variations include spatial inhomogeneities, primarily nonuniform external fields [1–3], environmental imperfections [4, 5], finite temperature effects such as a thermal velocity distribution [6–11], and fabrication infidelities in engineered systems [12–14]. Slow temporal fluctuations and shot-to-shot variations, also relevant to single-constituent systems, may as well manifest as inhomogeneous dephasing [10, 15–17]. In quantum information processing, these variations limit the qubit coherence time.

Traditionally, inhomogeneous dephasing is mitigated by using pulse-based protocols, such as echo sequences and various dynamical decoupling methods [18–20]. In these protocols, the system regains coherence only at discrete, pre-determined times. Several protocols of continuous dynamical decoupling have been studied [17, 21–24], all relying on strong resonant driving of the qubit transition. Such driving is not compatible with all systems and requires additional measures for eliminating the sensitivity to drive noise.

Here we propose and demonstrate an alternative approach for mitigating inhomogeneous dephasing. Our scheme employs off-resonance fields for continuously dressing the target state with an additional *sensor* state, which has an opposite and enhanced sensitivity to the same source of inhomogeneity. This admixture of a portion of the sensor state forms a protected, dephasing-free state. Notably, the dressing field is a continuous wave, providing continuous protection and not limiting the extraction of quantum information to predefined times.

Experimentally, we focus on optical excitations in thermal atomic ensembles. Storing and processing quantum information as collective excitations in atomic ensembles offers long coherence times [25–28], noiseless memory protocols [7, 29], remote entanglement [30–32], and the generation of non-classical light [33, 34]. Nevertheless, whether they are warm or ultracold, the atoms are never stationary; their inhomogeneous velocity distribution leads to dephasing of collective states formed by excitations with non-zero momentum transfer [10, 11, 35]. Such motional dephasing is a prevailing

decoherence mechanism, and still – except for several theoretical proposals [36, 37] – no general protocol for protection from motional dephasing has been realized to date.

In the following, we first present a general analysis of the protection scheme with either one or two dressing fields. We identify the minimal requirements and conditions for optimal protection. We show that introducing two dressing fields reduces not only the sensitivity to frequency variations, but also to fluctuations in the driving field, known as drive noise [21, 22, 38]. We then turn to the case study of motional dephasing in atomic ensembles. Our experimental realization is based on light storage in a fast ladder memory (FLAME) [7], using the retrieval efficiency as a measure of atomic coherence [39]. We demonstrate complete cancellation of motional dephasing, prolonging the memory lifetime, and verify the scaling of optimal conditions for protection. We further confirm that the double-dressing scheme, in contrast to the single-dressing scheme, introduces no global phase rotation and is thus less sensitive to drive noise, providing complete and robust continuous protection.

Continuous protection using a sensor state

Consider a qubit comprising the states $|\downarrow\rangle$ and $|\uparrow\rangle$, whose transition frequency experiences an inhomogeneous shift δ [Fig. 1(a)]. We require that one of these states, here chosen to be $|\uparrow\rangle$ without loss of generality, can be coupled by an external dressing field to a third state $|S\rangle$, which acts as a sensor. We further require that the overall frequency difference between $|\downarrow\rangle$ and $|S\rangle$ be sensitive to the same source of inhomogeneity, such that it experiences an opposite and possibly larger shift, $-s\delta$, where s is the sensitivity factor. For example, in the case of motional dephasing, s is the ratio between the Doppler widths of the transitions $|\downarrow\rangle - |S\rangle$ and $|\downarrow\rangle - |\uparrow\rangle$, and, in the case of magnetically sensitive transitions, s is the ratio between their magnetic moment differences. If the above requirements are satisfied, the dressing field can be tuned to protect the qubit from inhomogeneous dephasing.

We begin by considering a single dressing field with Rabi

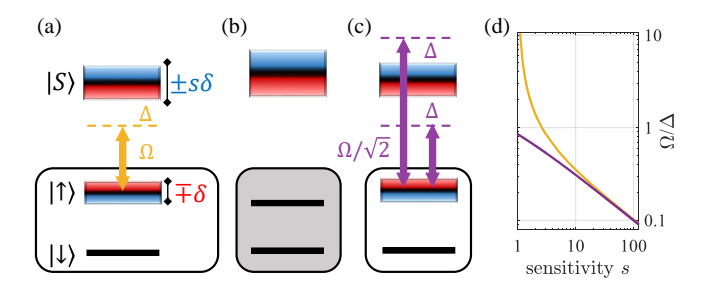


Figure 1. Continuous protection of a quantum state. (a) Without protection, the transition frequency of the qubit $|\downarrow\rangle - |\uparrow\rangle$ is shifted by δ due to some source of inhomogeneity, while an auxiliary sensor state $|S\rangle$ experiences an opposite and possibly larger shift $-s\delta$. A single field with Rabi frequency Ω and detuning Δ dresses the qubit with the sensor state. (b) A fully protected qubit is formed under conditions of optimal dressing. The transition frequency of the protected qubit is slightly altered by the mean light shift. (c) Applying two dressing fields of equal intensities and opposite detunings further eliminates the mean shift and reduces the sensitivity of the protected qubit to dressing noise. (d) Optimal dressing ratio Ω/Δ as a function of the sensitivity parameter s for the single dressing (orange) and double dressing (purple) schemes.

frequency Ω and detuning Δ [Fig. 1(b)]. The states $|\uparrow\rangle$ and $|S\rangle$ are mixed, forming dressed states. With respect to $|\downarrow\rangle$, the states $|S\rangle$ and $|\uparrow\rangle$ are inhomogeneously shifted by $[\Delta + \delta(s-1)]/2 \pm \sqrt{[\Delta + (s+1)\delta]^2/4 + \Omega^2}$. Optimal protection is achieved when the qubit transition frequency is insensitive to variations in δ to first order, which occurs when

$$\Omega^2/\Delta^2 = s/(s-1)^2. \tag{1}$$

This condition is shown in Fig. 1(d) by the orange line. Since the ratio Ω^2/Δ^2 determines the magnitude of mixing between the bare states, the larger the sensitivity factor s is, the smaller the portion of $|S\rangle$ admixed into $|\uparrow\rangle$ at optimal protection.

For $s\gg 1$, the dressed state frequency-shift takes the form of a light shift: $\Omega^2/(\Delta-s\delta)\approx (\Omega^2/\Delta)[1+s\delta/\Delta+O(s\delta/\Delta)^2]$. It is the first-order term $(\Omega/\Delta)^2s\delta$ which counteracts the inhomogeneous shift δ when condition (1) is fulfilled. Given a distribution of inhomogeneous shifts δ of width σ , a dressing field detuning $\Delta\gg s\sigma$ allows efficient protection for practically all δ . This regime has been recently used for narrowing and enhancement of spectral lines [6, 8].

A caveat of the single-dressing scheme is the mean, zeroth-order shift Ω^2/Δ added to the transition frequency of the protected qubit. This shift rotates the qubit phase in time, imparting sensitivity to noise in the drive field Ω . To avoid this, two dressing fields at two equal and opposite detunings $\pm \Delta$ should be used [Fig. 1(c)]. Their mean shifts are opposite in sign and thus cancel. In fact, as all even-order terms cancel, a protection up to third order in δ/Δ is achieved. The above arguments carry on to any s. For a general solution with more than one dressing field, we use the Magnus expansion of the time-dependent Hamiltonian and find the condition under which the transition frequency is insensitive to variations in δ to first and second order:

$$J_0(2\sqrt{2}\Omega/\Delta) = (s-1)/(s+1),$$
 (2)

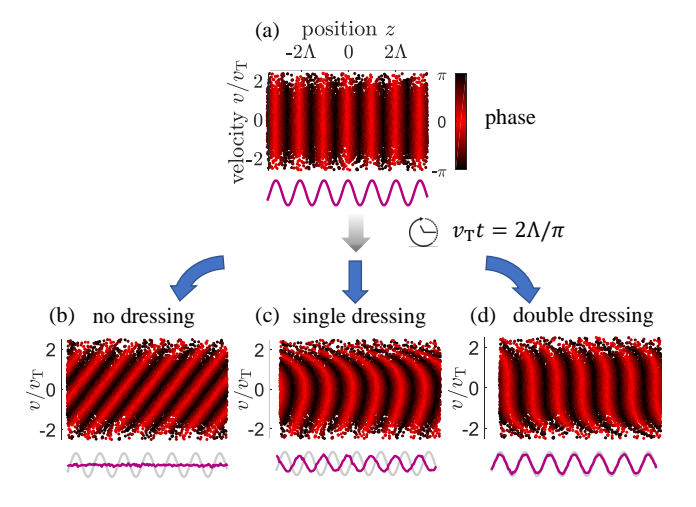


Figure 2. Motional dephasing and protection of a spin wave. (a) Position-velocity representation of a collective excitation (spin wave), generated, e.g., by light storage in a two-photon bi-chromatic transition. The collective state has a spatially dependent phase with a wavelength Λ (top), clearly apparent when the real part of the spinwave is averaged over all velocities (purple, bottom). (b) Thermal atomic motion (mean velocity v_T) at time $t = 2\Lambda/(\pi v_T)$ after the initial excitation. Averaging over velocities results in decoherence of the collective state. (c) In the presence of a single dressing field, atoms with different velocities experience different light shifts, and the spatial coherence is maintained up to second order in velocity. The zeroth-order term introduces a global phase shift, evident when comparing the spin wave (purple) to its original form (gray). (d) When two dressing fields are applied, the protection is up to third order in velocity (thus covering a wider velocity range), and no global phase shift is introduced. Calculations are performed with s = 110, $\Delta = 4v_T/\Lambda$, and optimal Ω from Eqs. (1) and (2).

where J_0 is the zeroth-order Bessel function (see Supplementary Information for the full derivation). Equation (2) converges to Eq. (1) for $s \gg 1$, but Ω/Δ scales more favorably with s for small s, such that less Rabi frequency and less mixing are required with double dressing [see Fig. 1(d)].

Motional dephasing

Initializing an ensemble of atoms in a collective state is typically done by optical excitation. When the wavevector $k=2\pi/\Lambda$ of the collective excitation is nonzero, a spatial phase $e^{i(2\pi/\Lambda)z}$ is imprinted on the atoms, as illustrated in Fig. 2(a). In multi-photon transitions, the excitation wavevector is the vectorial sum of the participating fields' wavevectors. For a single excitation, the collective state can be written as a spin wave $|W\rangle = \frac{1}{\sqrt{N}} \sum_j e^{i(2\pi/\Lambda)z_j} |\uparrow\rangle_j \langle\downarrow|_j |G\rangle$, where z_j is the position of atom j at storage time t=0, and $|G\rangle = \prod_j |\downarrow\rangle_j$ is the initial collective ground state. When the atoms due to their thermal velocity to a different position $z_j + v_j t$, atoms with different velocities carry the original phase to different positions along the spin wave [Fig. 2(b)]. The resulting

state is

$$|W'(t)\rangle = \sum_{j} e^{i(2\pi/\Lambda)(z_j - v_j t)} |\uparrow\rangle_j \langle\downarrow|_j |G\rangle,$$
 (3)

whose overlap with $|W\rangle$ determines the coherence of the spin wave and thus the retrieval efficiency of light into the phase-matched direction $\eta(t)/\eta(0) = |\langle W|W'(t)\rangle|^2 = e^{-\sigma^2t^2/2}$ [35]. Here, the width of the inhomogeneous shift is $\sigma = 2\pi v_{\rm T}/\Lambda$, where $v_{\rm T}$ is the atomic thermal velocity.

To apply the continuous protection scheme in the case of motional dephasing, we dress the spin-wave with a sensor state which has large and opposite sensitivity to velocity. This is achieved by an optical transition whose wavevector is larger than $2\pi/\Lambda$. The frequency shift of the qubit transition due to the dressing field depends on the atom velocity via the Doppler effect and, for optimal dressing, exactly cancels the bare motional dephasing, rendering a velocity-insensitive state. Remarkably, as shown in Figs. 2(c,d), although the atoms are constantly in motion during the evolution of the state, the spin-wave correlations between position and phase are predominantly maintained.

Apart from protecting against dephasing of the spin wave (when $|W\rangle \rightarrow |W'\rangle$), as quantified by the light retrieval efficiency, we are interested in protecting a general qubit $\alpha|G\rangle + \beta|W\rangle$. This qubit is formed, for instance, by mapping a photonic qubit $\alpha|0\rangle + \beta|1\rangle$, where $|0\rangle$ and $|1\rangle$ are photon number states, onto atomic collective states. Decoherence of $|W\rangle$ would naturally lead to decoherence of the qubit, but so will global phase fluctuations (of β/α) [40]. The double dressing scheme, which does not introduce global phase rotations that vary with drive noise, is therefore advantageous for robust protection of a qubit.

Experimental realization

To demonstrate and study the continuous protection against motional dephasing, we probe the coherence decay of a collective excitation in a hot atomic vapor, utilizing storage and retrieval of light. We employ the FLAME protocol [7] to store 1.8-ns (FWHM) signal pulses (with ~ 0.5 photons per pulse) on two-photon excitations [Fig. 3(a)] in a 5-mm-long cell of thermal ⁸⁷Rb vapor at 98°C. The $|\uparrow\rangle$ and $|\downarrow\rangle$ states reside in the levels $5S_{1/2}$ and $5D_{5/2}$ respectively. The two states are coupled via a two-photon transition, detuned by 1.4 GHz from the intermediate level $5P_{3/2}$ [$|i\rangle$ in Fig. 3(a)]. The temporal decay of the spatial coherence is probed by retrieving the collective excitation with a second control pulse after a storage time τ_s and measuring the retrieval efficiency η [Fig. 3(c) top]. To measure the phase difference between incoming and retrieved signal, we store slightly longer signal pulses (4-ns FWHM) and interfere them with reference pulses shifted by 380 MHz which do not traverse the atomic vapor [Fig. 3(c) bottom]. The homogeneous lifetime of the excitation (~ 115 ns) is limited by the $5D_{5/2}$ radiative lifetime and by the transit time of atoms through the signal beam waist (see Methods).

The wavevectors for the signal and control transitions are respectively $k_s = 2\pi/0.78~\mu\text{m}^{-1}$ and $k_c = 2\pi/0.776~\mu\text{m}^{-1}$,

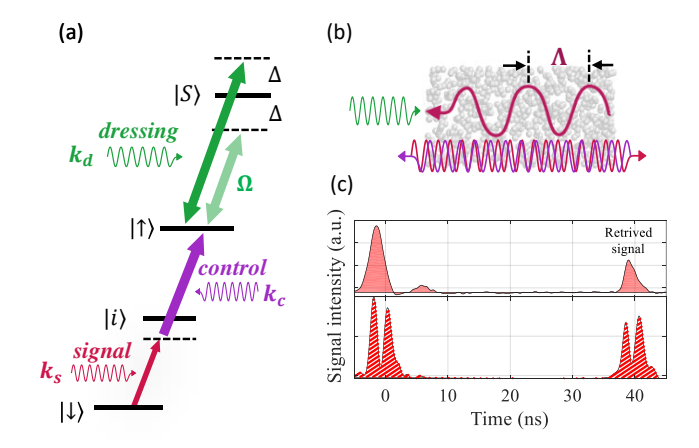


Figure 3. Experimental realization of continuous protection from motional dephasing (a) Light storage scheme: Counter-propagating pulses of a strong control field and a weak signal field with wavevectors k_c and k_s couple the ground state $|\downarrow\rangle$ to the excited state $|\uparrow\rangle$ through an intermediate state $|i\rangle$. A dressing beam with wavevector k_d couples $|\uparrow\rangle$ to the sensor state $|S\rangle$ with Rabi frequency Ω and detuning Δ . (b) The signal and control pulses generate a collective excitation with wavevector $2\pi/\Lambda = k_s - k_c$. A second control pulse maps this excitation back to a signal pulse. (c) Typical data traces when the incoming and retrieved signal are either directly measured (top) or interfered with a reference pulse to measure the phase of the signal (bottom).

giving an excitation wavelength $\Lambda=2\pi/(k_{\rm s}-k_{\rm c})=151~\mu{\rm m}$ [Fig. 3(b)]. The Gaussian distribution of velocities with a thermal velocity $v_T=188$ m/s results in an inhomogeneous dephasing of the collective state over about 100 ns. Protection during storage is obtained by a field with wavevector $k_{\rm d}=2\pi/1.274~\mu{\rm m}^{-1}$, propagating along the direction of the signal field and weakly dressing the state $|\uparrow\rangle$ with the state $|S\rangle=28F_{7/2}$. The sensor transition $|\downarrow\rangle-|S\rangle$ has an opposite and enhanced velocity-sensitivity $s\approx110$ compared to that of the two-photon transition $|\downarrow\rangle-|\uparrow\rangle$, such that weak dressing is sufficient to form a velocity-insensitive collective state.

We quantify the effect of protection by measuring the retrieval efficiency η for different storage times, with no dressing field, with a single dressing field, and with a double dressing field, as shown in Fig. 4. In the absence of dressing fields, the decay of efficiency with time has both exponential and Gaussian components, corresponding respectively to homogeneous and inhomogeneous dephasing. With a single dressing field, the inhomogeneous component is partially removed, while with the double dressing field, it vanishes almost completely (the residual inhomogeneous dephasing rate could not be faithfully extracted from the data). As a result, we observe an increase of over an order of magnitude in retrieved signal at long storage times. For storage times much shorter than the homogeneous decay rate, we measure a slight decrease in efficiency in the double-dressing case. This is consistent with an increase of $\leq 25\%$ in the homogeneous decay rate, which we attribute to resonant scattering due to EOM drifts and to the dressing beam inhomogeneity (see Methods).

To further study the optimal conditions for continuous pro-

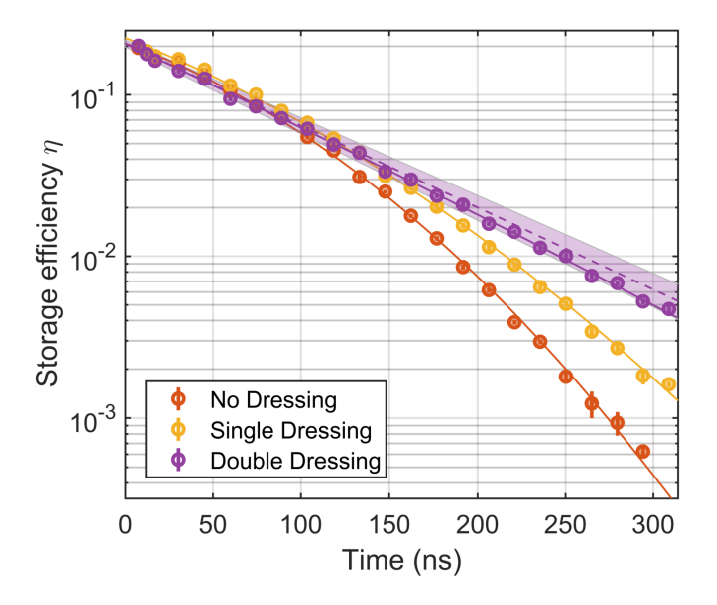


Figure 4. Protection of a collective excitation from inhomogeneous dephasing, quantified by memory retrieval efficiency. Solid lines are fit to a model accounting for both homogeneous and inhomogeneous dephasing. With double dressing, the decay is predominantly homogeneous; the dashed line marks the homogeneous component of the fitted decay model, with surrounding shaded area representing fit uncertainty. The dressing field detunings $|\Delta|$ =350 MHz and Rabi frequencies $\Omega=35$ MHz (double dressing) and $\Omega=28$ MHz (single dressing) were chosen to minimize the inhomogeneous dephasing.

tection, we vary the double-dressing parameters Ω and Δ and measure the retrieval efficiency at t=250 ns, which without protection drops to $\eta(250 \text{ ns}) \simeq 10^{-3}$. Figure 5(a) shows the significant gain in the retrieval efficiency when applying the dressing fields. We find that the dressing should be detuned by $\Delta > s\sigma$ for efficient protection (here $s\sigma=140$ MHz) and that the improvement with Δ saturates at a few $s\sigma$. Substantial gain in retrieval efficiency is obtained over a large range of dressing powers, and we find that the tolerance around the optimal Rabi frequency $\Omega_{\rm opt}(\Delta)$ is quite large. We validate the protection condition (2) by comparing in Fig. 5(b) the predicted ratio Ω/Δ to the measured ratio $\Omega_{\rm opt}(\Delta)/\Delta$. Excellent agreement is found for large detunings.

An important property of any protection or dynamical decoupling technique is the global phase introduced by the driving fields and its dependence on their intensities. Measurements of this dependence for both single and double dressing are shown in Fig. 5(c). For single dressing, we find indeed that the phase shift scales linearly with the mean light shift Ω^2/Δ [41], yielding a sensitivity to drive noise of \sim 0.4 mrad/MHz². This is in contrast to the double dressing protection, where we measure essentially no added phase and no dependence on the dressing intensity or on the storage time.

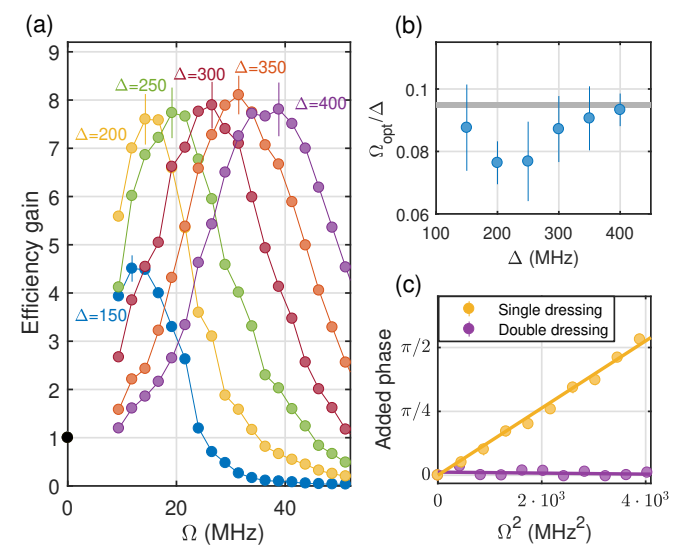


Figure 5. **Dependency of efficiency and global phase on the dressing parameters.** (a) Gain in retrieval efficiency achieved by double dressing, for a storage time of 250 ns, versus dressing Rabi frequency Ω , for different detunings Δ . For $\Delta \geq 200$ MHz, an 8-fold gain is achieved. (b) The ratio $\Omega_{\rm opt}/\Delta$, where $\Omega_{\rm opt}$ is the Rabi frequency maximizing the gain for each Δ , compared to the model prediction $2^{-3/2}J_0^{-1}[(s-1)/(s+1)] \approx s^{-1} \approx 0.095$ (solid line). (c) Global phase accumulated due to the dressing fields during a storage time of 40 ns. Here $\Delta = 480$ MHz. Solid lines are linear fits. For double dressing, the added phase is zero (up to the experimental uncertainty) and independent of the dressing intensity.

Discussion

The presented protection scheme is akin to continuous dynamical decoupling but distinct in several aspects. Our protecting fields do not couple the two states comprising the qubit, but rather couple one of them to an external state. They are preferably off-resonant, and the overall protection improves with further detuning. In continuous dynamical decoupling, on the other hand, the protecting fields drive the qubit transition, often resonantly, exposing it directly to drive noise δ_{Ω} when the field amplitude fluctuates $\Omega \to \Omega + \delta_{\Omega}$. Moreover, if δ fluctuates in time, the fluctuation bandwidth over which the protection is effective is limited by the available Rabi frequency [42]. In our scheme, the bandwidth is fundamentally limited by the detuning (or the effective Rabi frequency $\sqrt{4\Omega^2 + \Delta^2}$), which can be made much larger given the same limited power, especially with large sensitivity s (for which $\Delta \gg \Omega$)

In Table I, we present the effectiveness of the different protection schemes in terms of the residual, higher-order, sensitivities to inhomogeneous shift $O(\delta^2), O(\delta^3)$; to Rabi frequency fluctuations $O(\delta_\Omega)$; and to cross-terms of the two $O(\delta\delta_\Omega)$. For a single dressing field, an enhanced sensitivity $s\gg 1$, earned from utilizing a sensor state, affords for protection by a far-detuned dressing field, thus reducing sensitivity to drive noise to δ_Ω/\sqrt{s} . Further suppression of drive noise is achieved with double dressing, which we find to be insen-

Table I. Leading residual sensitivities of the qubit transition frequency: first-order in the drive noise (δ_{Ω}) , second- and third- order in the inhomogeneous shift (δ^2, δ^3) and the cross-term $(\delta_{\Omega} \cdot \delta)$. For the double dressing scheme, exact numerical factors depend on the experimental realization, including the phase between the two fields. These factors and their exact derivation are given in the supplementary information.

	single o	dressing	double dressing					
	$O(\delta_{\Omega})$	$O(\delta^2)$	$O(\delta_{\Omega})$	$O(\delta^2)$	$O(\delta\delta_{\!\Omega})$	$O(\delta^3)$		
s = 1	δ_{Ω}	$\frac{1}{2} \frac{\delta^2}{\Omega}$	0	0	$\sim 1 rac{\delta \delta_{\Omega}}{\Omega}$	$\sim rac{1}{2}rac{oldsymbol{\delta}^3}{\Omega^2}$		
$s\gg 1$	$\frac{2}{\sqrt{s}}\delta_{\Omega}$	$\sqrt{s}\frac{\delta^2}{\Omega}$	0	0	$2\frac{\delta\delta_{\Omega}}{\Omega}$	$\sim s \frac{\delta^3}{\Omega^2}$		

sitive to drive noise to leading order $O(\delta_\Omega)$ [also supported by the measurements in Fig. 5(c)]. Our analysis additionally shows that the double dressing removes sensitivity to inhomogeneous shifts up to $O(\delta^3)$. The remaining sensitivity scales inversely with Rabi frequency or with detuning, but we note that it scales unfavourably with the sensitivity factor s.

For a sensor state with sensitivity equal to that of the qubit state, s=1, the single dressing protection condition [Eq. (1)] requires a resonant field $\Delta=0$, which results in two, equally mixed, protected states. The double dressing scheme also generates two protected states in this case (see Supplementary Information), without the need for resonant driving. The s=1 case resembles the case of a two-level system, where the condition (2) provides for intrinsic dynamical decoupling in bichromatic entangling gates with trapped ions [38].

Our approach is particularly suitable for protection from motional dephasing of a collective state stored in an atomic ensemble, where limited solutions were suggested to date. Notably, for two-photon excitation to Rydberg states, the wavevector mismatch leads to decoherence times of microseconds for cold atoms and about a nanosecond for hot atoms [10, 43, 44]. This major limiting factor on the performance of quantum gates and sources could be tackled by identifying suitable sensor transitions and implementing the continuous protection scheme.

In conclusion, we have introduced and demonstrated a new scheme for protection from inhomogeneous dephasing, which is continuous, efficient, and robust to drive noise. The minimal requirements outlined in this paper may be found across numerous systems where a multi-level structure exists. For example, in systems suffering from sensitivity to magnetic field fluctuations, an auxiliary level with larger landé *g*-factor and opposite spin may be harnessed as a good sensor state. We have introduced a simple, yet exact, condition for optimal protection in any such general system.

Our experimental demonstration confirms the validity of the scheme by eliminating the inhomogeneous dephasing of a collective excitation in a gas of thermal atoms. Remarkably, this is achieved not through time-reversal of the process of dephasing or the direction of atomic motion, but through continuously maintaining the original position-dependent phases of atoms which move randomly to different positions.

The compatibility of this scheme to various protocols of quantum information processing, including gates and measurements, requires further research. It could provide an important tool for these applications operating with either single-constituent qubits or with collective quantum states of ensembles.

Methods

Experimental design. – The setup comprises a 780 nm distributed Bragg reflector (DBR) diode laser, serving as the signal beam, and a 776 nm external cavity diode laser (ECDL) amplified by a tapered amplifier (TA), serving as the control beam. The signal laser is offset-locked to a master ultra-stable fiber laser using a fast beat-note detector. The control laser is locked to a two-photon absorption feature in a reference cell when overlapped with the master laser, where the latter is frequency shifted by a fiber electro-optic phase modulator (EOPM). The signal field is amplitude modulated in time by two fiber electro-optic amplitude modulators (EOAM) to carve a Gaussian pulse of 1.8 ns FWHM, with a combined extinction ratio of 1:3000. The control field is amplitude modulated by two Pockels cells (PCs), generating pulses of 2.5 ns FWHM with an extinction ratio of 1:1000. The repetition rate of the experiment is set by that of the PCs to 100 kHz. After the modulators, the control beam is passed through a tilted filter (Semrock LL01-780-12.5) functioning as a 776 nm bandpass, filtering out other frequencies that might be produced in the TA. Both beams are passed through single mode fibers (SMF), aligned with each other in a counter-propagating geometry, and overlapped at the center the vapor cell. The signal beam is focused down to $w_0 = 85 \mu m$, while the control beam is focused down to $w_0 = 200 \ \mu m$. Both beams are σ^+ polarized, and we optically pump all atoms to the stretched state, a combination which guarantees purely orbital transitions and greatly simplifies the multi-level structure of the atomic vapor. The optical pumping is realized by a 'pump' and a 'repump' at 795 nm, both σ^+ polarized, and separated from each other by 6.8 GHz, such that the pump (repump) is resonant with the $F = 2 \rightarrow F' = 2$ ($F = 1 \rightarrow F' = 2$) transition of the rubidium D1 line. The pump (repump) beam power at the vapor cell is 300 mW (200 mW). The pump beams are 1.2 mm wide and are directed at a small angle with respect to the control beam. The 5-mm-long ⁸⁷Rb vapor cell is anti-reflection coated for 780-1064 nm. It is heated to 72°C at its coldest spot and 98°C at its hottest spot using two electrical current heaters, to set a Rb density of 6.5×10^{11} cm⁻³ and an optical depth OD ≈ 5 . We obtain $OD \approx 8.5$ with continuous optical pumping. After the cell, the signal beam is passed through a polarizing beamsplitter and two 780 nm bandpass filters to filter out any residual 776 nm and 795 nm components. It is then coupled to a SMF acting as a spatial filter, removing most of the spatially incoherent fluorescence emitted from the cell at 780 nm. The SMF is coupled either to a fast linear avalanche photo detector (APD) with bandwidth of 1 GHz, or to a single photon counting module (SPCM) connected to a time tagger with time bins of 100 ps.

Dressing fields generation.—The dressing beam is produced by a 1274 nm ECDL and is then passed through both an EOAM and an EOPM. For the double dressing protection scheme, the EOPM is modulated by a square wave electronic signal (with fast, 70 ps, rise/fall time), generating dominant first-order side bands comprising 78% of the total output power and a vanishingly small carrier (0.2%). The dressing beam is then amplified by an O-band booster optical amplifier (Thorlabs BOA1130S) and further amplified by a TA. The dressing laser frequency is stabilized to a wavelength meter with 1 MHz resolution (High-Finesse WS8-IR1). The dressing beam is combined with the signal beam on a dichroic mirror and focused to $w_0 = 200 \mu \text{m}$ in the vapor cell. It is also σ^+ polarized, thus coupling only to the stretched state.

Homogeneous dephasing in the experiment.- Under the protection condition, with a single dressing field and, more significantly, with a double dressing field, we measure a small increase in the homogeneous dephasing rate (of up to 25%). One may attribute such an increase to a fraction Ω^2/Δ^2 of the homogeneous dephasing rate of the sensor state which is added to the qubit dephasing rate. The sensor state should thus be chosen such that its homogeneous dephasing is slow compared to the qubit dephasing. Indeed, we choose to work with a Rydberg atomic level $28f_{7/2}$, whose lifetime at T = 373 K is 12 μ s. I fact, the ground-sensor coherence is not limited by radiative lifetime, but rather by the transit time through the signal beam ($w_0 = 85 \mu m$), yielding a rate of ~ 0.3 MHz. However, the fraction Ω^2/Δ^2 of this rate is just 3 kHz, much smaller than the measured added dephasing rate. Other ground-sensor dephasing mechanisms in our case may include differential electric field sensitivity. We have tested this mechanism by trying different sensor states with significantly smaller polarizabilities (such as Rydberg P-states) and measured no significant change in added dephasing rate. This calls for different explanations, related to our specific experimental setup. For the double dressing scheme, the experimental realization (as detailed above) includes a single laser tuned to resonance and a fast squarewave phase modulation, whose imperfections result in a carrier intensity of $\Omega_{\text{carrier}}^2/\Omega^2=0.2(1)\%$. This corresponds to a calculated resonant scattering rate of 1.5(5) MHz at the optimal Rabi frequency of $\Omega = 35$ MHz (used for measuring the overall dephasing rate in the experiment). This can indeed account for the measured increase in the dephasing rate. For the single dressing scheme, the dressing beam's finite size $(w_0 = 200 \ \mu \text{m})$ results in a nonuniform light shift in the transverse plane with variations of order $0.1\Omega^2/\Delta \approx 0.35$ MHz, which is added to the dephasing rate. This mechanism can thus account for the increase in dephasing rate at this case. We thus conclude that technical limitations such as the extinction ratio of the EOPM in the double dressing scheme and the finite width of the dressing beam in the single dressing scheme are the main sources of added homogeneous dephasing under protection conditions. These limitations can be overcome by further improvements in the setup, for example by better temperature stabilization of the EOPM.

Phase measurements.— In order to measure the phase between the retrieved signal and the incoming light pulse, we generate two consecutive signal pulses and split the incoming signal with an acousto-optical modulator (AOM). The refer-

ence pulses, shifted by 380 MHz relative to the signal, are coupled into an optical fiber, acting as a delay line. The time difference between the consecutive pulses, the memory storage time, and the time delay in the delay line are all set to be identical. In this way, part of the incoming signal, which was not stored due to limited efficiency, is interfered with the first reference pulse and the retrieved signal is interfered with the second reference pulse. The phase difference between these two pulses, acquired in a single shot within tens of ns, is thus insensitive to interferometer drifts, which occur over a much longer time scale. We then average this value over hundreds of repetitions.

Author contributions—R.F., O.L., O.D., S.K., and E.P. contributed to the experimental design, construction, data collection and analysis of this experiment. I.C., R.F., O.L., and E.P. developed the theoretical framework supporting the experiment. E.P. and O.F. supervised the entire project. All authors discussed the results and contributed to writing the manuscript.

Competing interests—The authors declare no competing interests.

Acknowledgements— We acknowledge financial support by the Israel Science Foundation and ICORE, the European Research Council starting investigator grant QPHOTONICS 678674, the Pazy Foundation, the Minerva Foundation with funding from the Federal German Ministry for Education and Research, and the Laboratory in Memory of Leon and Blacky Broder. I.C. acknowledges support from Marie Skodowska-Curie grant agreement no. 785902.

- [1] Lepoutre, S. *et al.* Spin mixing and protection of ferromagnetism in a spinor dipolar condensate. *Phys. Rev. A* **97**, 23610 (2018).
- [2] Munowitz, M. & Pines, A. Multiple-quantum nuclear magnetic resonance spectroscopy. *Science* **233**, 525–531 (1986).
- [3] Kotler, S., Akerman, N., Glickman, Y., Keselman, A. & Ozeri, R. Single-ion quantum lock-in amplifier. *Nature* 473, 61–65 (2011). 1101.4885.
- [4] Pingault, B. *et al.* All-optical formation of coherent dark states of silicon-vacancy spins in diamond. *Physical Review Letters* **113** (2014). 1409.4069.
- [5] Cogan, D. et al. Depolarization of electronic spin qubits confined in semiconductor quantum dots. Phys. Rev. X 8, 041050 (2018).
- [6] Finkelstein, R. et al. Power narrowing: counteracting Doppler broadening in two-color transitions. New Journal of Physics 21, 103024 (2019). 1904.08529.
- [7] Finkelstein, R., Poem, E., Michel, O., Lahad, O. & Firstenberg, O. Fast, noise-free memory for photon synchronization at room temperature. *Science Advances* 4 (2018). 1708.01919.
- [8] Lahad, O. et al. Recovering the homogeneous absorption of inhomogeneous media. Physical Review Letters 123 (2019). 1904.06233.
- [9] Kaplan, A., Fredslund Andersen, M. & Davidson, N. Suppression of inhomogeneous broadening in rf spectroscopy of optically trapped atoms. *Physical Review A* 66, 4 (2002).
- [10] Levine, H. et al. High-fidelity control and entanglement of rydberg-atom qubits. Phys. Rev. Lett. 121, 123603 (2018).
- [11] Saffman, M. Quantum computing with atomic qubits and Rydberg interactions: Progress and challenges. *Journal of Physics B: Atomic, Molecular and Optical Physics* 49 (2016). 1605.05207.
- [12] Senellart, P., Solomon, G. & White, A. High-performance semiconductor quantum-dot single-photon sources. *Nature Nanotechnology* 11, 1026–1039 (2017).
- [13] Krantz, P. et al. A quantum engineer's guide to superconducting qubits. Appl. Phys. Rev 6, 21318 (2019).
- [14] Devoret, M. H. & Schoelkopf, R. J. Superconducting circuits for quantum information: An outlook (2013).
- [15] Manovitz, T., Shaniv, R., Shapira, Y., Ozeri, R. & Akerman, N. Precision Measurement of Atomic Isotope Shifts Using a Two-Isotope Entangled State. *Physical Review Letters* 123 (2019). 1906.05770.
- [16] Aharon, N., Drewsen, M. & Retzker, A. General scheme for the construction of a protected qubit subspace. *Physical Review Letters* 111 (2013). 1307.2933.
- [17] Bermudez, A., Schmidt, P. O., Plenio, M. B. & Retzker, A. Robust trapped-ion quantum logic gates by continuous dynamical decoupling. *Physical Review A - Atomic, Molecular, and Opti*cal Physics 85 (2012). 1110.1870.
- [18] Viola, L., Knill, E. & Lloyd, S. Dynamical decoupling of open quantum systems. *Physical Review Letters* 82, 2417–2421 (1999).
- [19] Khodjasteh, K. & Lidar, D. A. Fault-tolerant quantum dynamical decoupling. *Physical Review Letters* 95 (2005). 0408128.
- [20] Souza, A. M., Álvarez, G. A. & Suter, D. Robust Dynamical Decoupling for Quantum Computing and Quantum Memory (2011).
- [21] Fanchini, F. F., Hornos, J. E. & Napolitano, R. D. Continuously decoupling single-qubit operations from a perturbing thermal bath of scalar bosons. *Physical Review A* **75** (2007).

- [22] Tan, T. R. et al. Demonstration of a dressed-state phase gate for trapped ions. *Physical Review Letters* 110 (2013). 1301.3786.
- [23] Golter, D. A., Baldwin, T. K. & Wang, H. Protecting a Solid-State Spin from Decoherence Using Dressed Spin States. *Physical Review Letters* 113 (2014).
- [24] Stark, A. et al. Clock transition by continuous dynamical decoupling of a three-level system. Scientific Reports 8 (2018). 1805.09435.
- [25] Zhao, R. et al. Long-lived quantum memory. Nature Physics 5, 100–104 (2009).
- [26] Dudin, Y. O., Li, L. & Kuzmich, A. Light storage on the time scale of a minute. *Physical Review A Atomic, Molecular, and Optical Physics* **87** (2013).
- [27] Körber, M. et al. Decoherence-protected memory for a single-photon qubit. Nature Photonics 12, 18–21 (2018). 1712.03668.
- [28] Katz, O. & Firstenberg, O. Light storage for one second in room-temperature alkali vapor. *Nature Communications* 9, 2074 (2018).
- [29] Kaczmarek, K. T. et al. High-speed noise-free optical quantum memory. Physical Review A 97, 042316 (2018).
- [30] Julsgaard, B., Kozhekin, A. & Polzik, E. S. Experimental long-lived entanglement of two macroscopic objects. *Nature* 413, 400–403 (2001).
- [31] Krauter, H. et al. Deterministic quantum teleportation between distant atomic objects. Nature Physics 9, 400–404 (2013). 1212.6746.
- [32] Lettner, M. et al. Remote entanglement between a single atom and a bose-einstein condensate. Physical Review Letters 106 (2011). 1102.4285.
- [33] Duan, L. M., Lukin, M. D., Cirac, J. I. & Zoller, P. Long-distance quantum communication with atomic ensembles and linear optics. *Nature* 414, 413–418 (2001). 0105105.
- [34] Boyer, V., Marino, A. M., Pooser, R. C. & Lett, P. D. Entangled images from four-wave mixing. *Science* 321, 544–547 (2008).
- [35] Whiting, D. J., Sibalić, N., Keaveney, J., Adams, C. S. & Hughes, I. G. Single-Photon Interference due to Motion in an Atomic Collective Excitation. *Physical Review Letters* 118 (2017). 1612.05467.
- [36] Moiseev, S. A. & Kröll, S. Complete reconstruction of the quantum state of a single-photon wave packet absorbed by a doppler-broadened transition. *Physical Review Letters* 87 (2001).
- [37] Shi, X.-F. Suppressing Motional Dephasing of Ground-Rydberg Transition for High-Fidelity Quantum Control with Neutral Atoms. *Phys. Rev. Appl.* **13**, 24008 (2020).
- [38] Sutherland, R. T. et al. Versatile laser-free trapped-ion entangling gates. New Journal of Physics 21 (2019). 1810.08300.
- [39] Phillips, D. F., Fleischhauer, A., Mair, A., Walsworth, R. L. & Lukin, M. D. Storage of light in atomic vapor. *Phys. Rev. Lett.* 86, 783–786 (2001).
- [40] Schmidt-Eberle, S., Stolz, T., Rempe, G. & Dürr, S. Dark-time decay of the retrieval efficiency of light stored as a Rydberg excitation in a noninteracting ultracold gas. Tech. Rep. (2019). 1909.00680v1.
- [41] Parniak, M. et al. Quantum Optics of Spin Waves through ac Stark Modulation. Phys. Rev. Lett. 122 (2019). 1804.05854.
- [42] Stark, A. et al. Narrow-bandwidth sensing of high-frequency fields with continuous dynamical decoupling. Nat. Commun. 8, 1–6 (2017). 1706.04779.
- [43] Ripka, F., Kübler, H., Löw, R. & Pfau, T. A room-temperature single-photon source based on strongly interacting Rydberg

- atoms. Science 362, 446-449 (2018). 1806.02120.
- [44] Graham, T. M. et al. Rydberg-Mediated Entanglement in a Two-Dimensional Neutral Atom Qubit Array. Physical Review Letters 123 (2019).
- [45] Consider three states $|\psi_n\rangle$ (n=1,2,3) with energies $\hbar\omega_n(\delta^*)=\hbar(\omega_n^0+a_n\delta^*)$, arranged such that $a_1\leq a_2\leq a_3$. If $a_1=a_2$ or $a_2=a_3$, then the corresponding transition is already protected from dephasing due to changes in δ^* . Otherwise, denote $n_\pm=2\pm \mathrm{sign}(a_1-2a_2+a_3)$ and define $|\downarrow\rangle\equiv|\psi_2\rangle, |\uparrow\rangle\equiv|\psi_{n_-}\rangle, |S\rangle\equiv|\psi_{n_+}\rangle, \,\delta\equiv(a_2-a_{n_-})\delta^*, \,\mathrm{and}\,\, s\equiv(a_{n_+}-a_2)/(a_2-a_{n_-}).$ [46] Facchi, P., Lidar, D. A. & Pascazio, S. Unification of dynam-
- [46] Facchi, P., Lidar, D. A. & Pascazio, S. Unification of dynamical decoupling and the quantum zeno effect. *Phys. Rev. A* 69, 032314 (2004).
- [47] James, D. F. & Jerke, J. Effective hamiltonian theory and its applications in quantum information. *Canadian Journal of Physics* 85, 625–632 (2007).
- [48] Srinivas, R. et al. Trapped-ion spin-motion coupling with microwaves and a near-motional oscillating magnetic field gradient. Phys. Rev. Lett. 122, 163201 (2019).
- [49] Roos, C. F. Ion trap quantum gates with amplitude-modulated laser beams. *New Journal of Physics* **10**, 013002 (2008).

SUPPLEMENTARY INFORMATION: OPTICAL PROTECTION OF A COLLECTIVE STATE FROM INHOMOGENEOUS DEPHASING

Derivation of protection conditions and sensitivity analysis

Let $\{|\downarrow\rangle,|\uparrow\rangle,|S\rangle\}$ be a three-level system, comprising a qubit $\{|\downarrow\rangle,|\uparrow\rangle\}$ and a sensor state $|S\rangle$. Let the frequencies of the transitions $|\downarrow\rangle-|\uparrow\rangle$ and $|\downarrow\rangle-|S\rangle$ be inhomogeneously shifted, with the magnitude of the shifts linearly dependent on the same inhomogeneous variable δ . We assume (without loss of generality, see footnote [45]) that $|\downarrow\rangle-|\uparrow\rangle$ and $|\downarrow\rangle-|S\rangle$ shift to opposite directions and that $|\downarrow\rangle-|S\rangle$ is at least as sensitive as $|\downarrow\rangle-|\uparrow\rangle$ to the inhomogeneity. Hereafter, we take the ground state $|\downarrow\rangle$ as the frequency reference and examine the transition frequencies relative to it. In a frame rotating with the unshifted frequencies, the Hamiltonian in the subspace $\{|\uparrow\rangle,|S\rangle\}$ is given for any constituent in the ensemble as $(\hbar=1)$

$$H_0 = \delta \begin{pmatrix} -1 & 0 \\ 0 & s \end{pmatrix}. \tag{S1}$$

Here δ is a random (inhomogeneous) variable with a standard deviation σ , and the sensitivity parameter $s \ge 1$ is defined by construction. We aim to add coupling fields in this subspace that will render (at least one) protected state, *i.e.*, a dressed state with a reduced sensitivity to δ . Note that we do not explicitly use σ in the following; rather, it is implicitly understood that σ should substitute for δ when assessing the validity of various expansions in leading orders in δ .

S-.1. Protection by a single-tone dressing field

A single classical field that dresses the transition $|\uparrow\rangle - |S\rangle$ with a Rabi frequency Ω and detuning Δ yields the Hamiltonian

$$H = H_0 + \begin{pmatrix} \Delta & \Omega \\ \Omega & 0 \end{pmatrix}. \tag{S2}$$

By diagonalizing H, we obtain the new transition frequencies

$$\omega_{\pm} = \frac{1}{2} \left[\Delta + \delta (s - 1) \pm \sqrt{\left[\Delta + (s + 1) \delta \right]^2 + 4\Omega^2} \right]. \tag{S3}$$

By requiring a vanishing derivative with respect to δ of one of these frequencies $(d\omega/d\delta)|_{\delta\to 0}=0$, we obtain the protection condition [Eq. (1) in the main text]

$$\left(\frac{\Omega}{\Delta}\right)^2 = \frac{s}{(s-1)^2}.\tag{S4}$$

In the case of a sensor state with high sensitivity $s \gg 1$, this condition reduces to $(\Omega/\Delta)^2 = 1/s$.

An example for the spectrum of the two dressed states under the protection condition is shown in Fig. S1. For the general case $s \neq 1$, the two states $|\uparrow\rangle, |S\rangle$ are not equally mixed, and we obtain a single protected state. Conversely, when s=1, optimal protection is reached with a resonant dressing $\Delta=0$ and with the two states equally mixed, and therefore we obtain two protected states, which can be employed to form a qutrit. In this regime, our scheme is akin to the traditional two-level continuous dynamical decoupling (CDD) [46].

While protecting up to first order in δ , the single dressing field adds a qubit transition frequency shift of second-order in the inhomogeneous shift δ

$$\Delta\omega_{\delta^2} = \frac{s\delta^2}{\Omega} \frac{\sqrt{s}}{s+1},\tag{S5}$$

which is inversely proportional to the available Ω . In addition, the protection is subjected to drive noise in the form of amplitude fluctuations $\Omega \to \Omega + \delta_{\Omega}$, giving rise to a transition frequency shift

$$\Delta\omega_{\delta_{\Omega}} = 2\delta_{\Omega} \frac{\sqrt{s}}{s+1}.\tag{S6}$$

For high sensitivity $s \gg 1$, the drive noise is attenuated by $1/\sqrt{s}$, while the second-order inhomogeneous shift is enhanced by \sqrt{s} . These scalings are summarized in table S1 (left section) and compared to the residual transition frequency shifts under the other protection schemes, presented in the following sections.

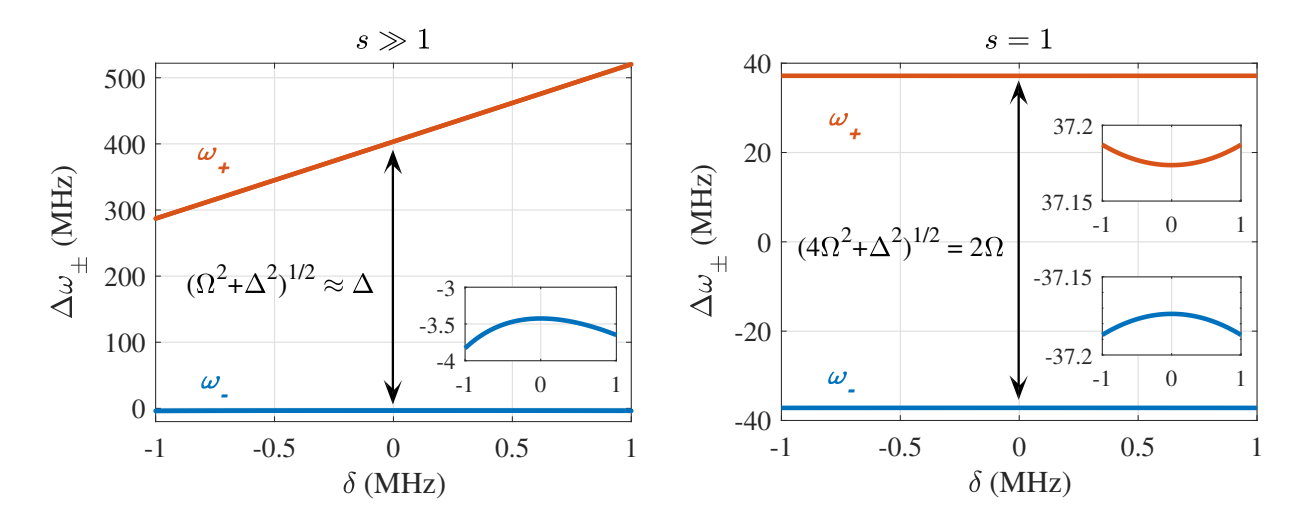


Figure S1. Dressed-state spectrum for a single-dressing protection. Transition frequency shift as a function of the inhomogeneous shift δ , after introducing a dressing field with Rabi frequency $\Omega=37$ MHz and detuning Δ . Left panel: For high sensor sensitivity ($s=110\gg1$), there exists one protected state (insensitive to δ to first order). The energy gap is dominated by the detuning $\Delta=400$ MHz, which is much larger than Ω . Right panel: For s=1, there exist two protected states. Optimal protection is achieved with a resonant dressing field ($\Delta=0$), and thus the energy gap is dominated by Ω . Insets magnify the spectrum near $\delta=0$, revealing the magnitude of the second-order shift.

Table S1. Higher-order corrections for the qubit transition frequency shifts: first-order in the drive noise ($O(\delta_{\Omega})$), second- and third- order in the inhomogeneous shift ($O(\delta^2)$, $O(\delta^3)$) and their cross-term ($O(\delta\delta_{\Omega})$).

	single-tone dressing		two-tone dressing				stepwise phase			
	$O(\delta_{\Omega})$	$O(\delta^2)$	$O(\delta_{\Omega})$	$O(\delta^2)$	$O(\delta\delta_{\Omega})$	$O(\delta^3)$	$O(\delta_{\Omega})$	$O(\delta^2)$	$O(\delta\delta_{\Omega})$	$O(\delta^3)$
s = 1	δ_{Ω}	$\frac{1}{2} \frac{\delta^2}{\Omega}$	0	0	$1.25 \frac{\delta \delta_{\Omega}}{\Omega}$	$(0.06\sim0.4)\frac{\delta^3}{\Omega^2}$	0	0	$\frac{\delta \delta_{\Omega}}{\Omega}$	$\frac{1}{2} \frac{\delta^3}{\Omega^2}$
$s\gg 1$	$\frac{2}{\sqrt{s}}\delta_{\Omega}$	$\sqrt{s}\frac{\delta^2}{\Omega}$	0	0	$2\frac{\delta\delta_{\Omega}}{\Omega}$	$s\frac{\delta^3}{\Omega^2}$	0	0	$2\frac{\delta\delta_{\Omega}}{\Omega}$	$\frac{6s}{5} \frac{\delta^3}{\Omega^2}$

S-.2. Protection by a two-tone dressing field

A dressing field comprising two tones with symmetric detuning $\pm \Delta$ around the $|\uparrow\rangle - |S\rangle$ transition can protect the $|\downarrow\rangle - |\uparrow\rangle$ transition better than a single-tone dressing, that is, up to higher orders in the inhomogeneous shift δ and in the drive noise δ_{Ω} . With this field, the time-dependent Hamiltonian in the rotating frame is given by $H(t) = H_0 + H_2(t)$, where

$$H_2(t) = \sqrt{2}\Omega\cos(\Delta t + \phi) \begin{pmatrix} 0 & 1 \\ 1 & 0 \end{pmatrix}, \tag{S7}$$

where ϕ is the phase between the two tones of the dressing at t = 0. The $\sqrt{2}$ factor appears above in order to maintain the overall dressing power as in the single-dressing scheme.

S-.2(a). Solution for
$$s \gg 1$$

Before presenting the general solution, we consider the limit $s \gg 1$. Since $\Delta \gg \Omega$, we can solve the time-dependent Hamiltonian using the effective Hamiltonian technique [47], where each field gives rise to a standard light shift,

$$H_{\pm\Delta} = \frac{\Omega^2/2}{\pm \Delta + \delta(s+1)} \begin{pmatrix} -1 & 0 \\ 0 & 1 \end{pmatrix} \approx \frac{\Omega^2}{\pm 2\Delta} \left(1 - \frac{s\delta}{\pm \Delta} + \left[\frac{s\delta}{\Delta} \right]^2 \right) \begin{pmatrix} -1 & 0 \\ 0 & 1 \end{pmatrix}. \tag{S8}$$

When summing both contributions $H \approx H_{+\Delta} + H_{-\Delta}$, we are left with only the odd orders in δ . The first order compensates for the inhomogeneous shift terms in the bare Hamiltonian H_0 when the protection condition

$$\frac{\Omega^2}{\Delta^2} = \frac{1}{s} \tag{S9}$$

is satisfied. This condition coincides with that of the single-dressing scheme [Eq. (S4)] for $s \gg 1$. However, unlike for single dressing, here the residual inhomogeneity is of third order in δ , as both the first and the second orders are elimniated. In addition, since the zeroth order of the light shift is eliminated as well, the double dressing scheme is also protected from the first-order contribution of the drive noise δ_{Ω} (the fluctuations in Ω). A general solution and a complete sensitivity analysis for the general case are presented below.

S-.2(b). Solution for general s using the Magnus expansion

We use the Magnus expansion to calculate both the exact protection condition for a general s and the remaining high-order noise contributions. We start by writing the bare Hamiltonian (S1) as

$$H_0 = \frac{\delta}{2} ([s-1] \mathbb{I} - [s+1] \sigma_z), \tag{S10}$$

where σ_z is the Pauli-z operator, and \mathbb{I} is the identity. To ease the derivation, we rotate the system around the y axis, such that $\sigma_x \to S_z$ and $\sigma_z \to -S_x$. The rotated Hamiltonian is

$$H_{y} = U_{y}(H_{0} + H_{2})U_{y}^{\dagger} = \frac{\delta}{2}\left[(s-1)\mathbb{I} + (s+1)S_{x}\right] + \sqrt{2}\Omega S_{z}\cos(\Delta t + \phi), \tag{S11}$$

Next, we move to a time-dependent rotating frame, utilizing $H_2(t)$ to construct the unitary rotation operator

$$U(t) = \exp\left(-\frac{i}{\hbar} \int_0^t U_y H_2(t) U_y^{\dagger} dt\right) = e^{-iS_z \sqrt{2}(\Omega/\Delta)[\sin(\Delta t + \phi) - \sin\phi]}$$
(S12)

and obtain the Hamiltonian in the interaction picture

$$H'_{y} = \frac{\delta}{2} \left[(s-1)\mathbb{I} + (s+1) \left(S_{+} e^{iz\left[\sin(\Delta t + \phi) - \sin\phi\right]} + \text{H.c.} \right) \right]$$
(S13)

with $z = 2\sqrt{2}\Omega/\Delta$.

Using the JacobiAnger expansion

$$e^{\pm iz\sin(\Delta t + \phi)} = \sum_{n = -\infty}^{\infty} J_n(z)e^{\pm in(\Delta t + \phi)},$$
(S14)

we expand Eq. (S13) in leading orders of the Magnus expansion. The first order reads

$$H^{(1)} = \frac{1}{t} \int_0^t H_y'(t_1) dt_1 = \frac{\delta}{2} \left[(s-1) \mathbb{I} + J_0(z) (s+1) \left(S_+ e^{-iz\sin\phi} + S_- e^{iz\sin\phi} \right) \right]. \tag{S15}$$

Since $(S_+e^{-iz\sin\phi} + S_-e^{iz\sin\phi})$ is a sum of Pauli matrices, it has two eigenvalues ± 1 . To find the protection condition [Eq. (2) in the main text], we require that the eigenvalues of $H^{(1)}$ be independent of δ , which occurs when

$$J_0(z) = \frac{s-1}{s+1}. ag{S16}$$

For $s \gg 1$, the condition (S16) can be expanded to the leading order in z:

$$1 - \frac{z^2}{4} + O(z^4) = 1 - \frac{2}{s} + O(s^{-2}), \tag{S17}$$

where we recover the previous (light shift) condition (S9). For s=1, as before, the first-order dependence on δ vanishes for both dressed states, and we obtain two protected states. Therefore, again, the whole three-level system is protected [38, 48]. For a general $s \neq 1$, the protected dressed state is rotated by $z \sin \phi$ around the x axis in the $\{|\uparrow\rangle, |S\rangle\}$ subspace,

$$|P\rangle = \exp\left(-i\sigma_x \frac{z\sin\phi}{2}\right)|\uparrow\rangle.$$
 (S18)

When the fields are in-phase ($\phi = 0$), or for high sensitivity $s \gg 1$ (as in our experiment), the dressed state is approximately the bare state $|\uparrow\rangle$. Otherwise, in order to efficiently couple to the protected dressed state, the phase term $(z\sin\phi)/2$ needs to be well defined, and it would determine the adiabatic condition for switching on and off of the protection fields [49].

To find the higher-order noise terms, it is beneficial to make the distinction between noise terms that are parallel and perpendicular to the dressed-state basis. For brevity, we define the pauli-x operator in the $z\sin\phi$ -dependent (dressed state) basis as $F_x = \left(S_+ e^{-iz\sin\phi} + S_- e^{iz\sin\phi}\right)$ an rewrite Eq. (S15) as

$$H^{(1)} = \frac{\delta(s-1)}{2} \left(\mathbb{I} + F_x \right). \tag{S19}$$

The protected dressed state is the eigenstate of F_x with the eigenvalue -1. The perpendicular pauli operators are $F_y = -i(S_+e^{-iz\sin\phi} - S_-e^{iz\sin\phi})$, and $F_z = S_z$.

We begin with the cross term of the inhomogeneous shift δ and the drive amplitude fluctuations δ_{Ω} ,

$$H_{\delta \cdot \delta_{\Omega}}^{(1)} = \left[-J_1(z)F_x + \sin\phi J_0(z)F_y \right] \frac{2\sqrt{2}}{\Delta} \frac{s+1}{2} \delta \delta_{\Omega}. \tag{S20}$$

With respect to Eq. (S19), this noise term has both a parallel ($\propto F_x$) and a perpendicular ($\propto F_y$) contributions. Notably, the perpendicular contribution vanishes when $\phi \to 0$. For a general ϕ , we examine the limits s = 1 and $s \gg 1$:

• For s = 1, according to condition (S16), we set $J_0(z) = (s-1)/(s+1) = 0$ and are left with only the parallel term

$$\Delta\omega_{\delta\cdot\delta_{\Omega}} \approx 1.25 \frac{\delta\delta_{\Omega}}{\Omega}.$$
 (S21)

• For $s \gg 1$, we approximate the perpendicular term as $H^{(1)}_{\delta \cdot \delta_{\Omega}, \perp} \approx \sin \phi \sqrt{2s} \delta(\delta_{\Omega}/\Omega) F_y$. From Eq. (S19), if the energy gap $\Delta \omega = \delta(s-1)$ in the F_x direction is larger than the perpendicular F_y noise, and assuming $\sin \phi \sqrt{2/s} (\delta_{\Omega}/\Omega) \ll 1$, then the perpendicular noise manifests only as a small perturbation $\Delta \omega_{\delta \cdot \delta_{\Omega}, \perp} \propto \delta(\delta_{\Omega}/\Omega)^2$. Therefore, the leading contribution is the parallel term

$$\Delta\omega_{\delta\cdot\delta_{\Omega}} = 2\frac{\delta\delta_{\Omega}}{\Omega}.\tag{S22}$$

We now turn to evaluate the residual second-order contribution of the inhomogeneous shift. We take the next order in the Magnus expansion using the Jacobi-Anger expansion (S14)

$$H^{(2)} = -\frac{i}{2t} \int_0^t dt_1 \int_0^{t_1} dt_2 \left[H_y'(t_1), H_y'(t_2) \right] = -2 \left[\frac{\delta(s+1)}{2} \right]^2 J_0(z) \sum_{n \neq 0} \frac{J_n(z) \cos n\phi}{n\Delta} F_z$$
 (S23)

and again examine different s regimes:

- For s = 1, we have $J_0(z) = 0$, and therefore $H^{(2)} = 0$ for any ϕ .
- For general s > 1, $H^{(2)}$ contains a perpendicular (F_z) contribution with respect to Eq. (S19), which vanishes for $\phi \to \pi/2$. For a general ϕ , this perpendicular term is not vanishing.
- In the limit $s \gg 1$ and $z/2 = \sqrt{2/s} \ll 1$, we expand $H^{(2)}$ to leading orders

$$H^{(2)} \approx -\left[\frac{\delta(s+1)}{2}\right]^2 \frac{2z\cos\phi}{\Delta} F_z \approx -\frac{\delta^2 s\sqrt{2s}\cos\phi}{\Delta} F_z \approx -\frac{\delta^2 s\sqrt{2}\cos\phi}{\Omega} F_z. \tag{S24}$$

Once again, if the energy gap of $H^{(1)}$ [Eq. (S19)] is larger than this perpendicular term and assuming $\sqrt{2}\cos\phi\delta\ll\Omega$, we get only a small, third-order correction

$$H^{(2)} \approx 2 \frac{s \delta^3 \cos^2 \phi}{\Omega^2} F_x. \tag{S25}$$

We find for both $s \gg 1$ and s = 1 that the double-dressing scheme eliminates the first- and second- order contributions of the inhomogeneous shift. Note that when $s \neq 1$ but not large and $\phi \neq \pi/2$, there will be a non-vanishing second order contribution.

To fully evaluate the contribution of the inhomogeneous shift to third order, we take the third order of the Magnus expansion

$$H^{(3)} = -\frac{1}{6t} \int_0^t dt_1 \int_0^{t_1} dt_2 \int_0^{t_2} dt_3 \left(\left[H_y'(t_1), \left[H_y'(t_2), H_y'(t_3) \right] \right] + \left[H_y'(t_3), \left[H_y'(t_2), H_y'(t_1) \right] \right] \right). \tag{S26}$$

For a general s, we obtain

$$H^{(3)} = \left[\frac{\delta(s+1)}{2}\right]^{3} \sum_{n>0} \left\{ \frac{4(J_{2n}(z))^{3}}{(2n\Delta)^{2}} \cos 2n\phi F_{x} - \frac{4(J_{2n-1}(z))^{3}}{((2n-1)\Delta)^{2}} \sin(2n-1)\phi F_{y} \right\}$$

$$-\left[\frac{\delta(s+1)}{2}\right]^{3} J_{0}(z) \sum_{n>0} \frac{2(2+\cos 2n\phi)(J_{n}(z))^{2}}{(n\Delta)^{2}} F_{x}$$

$$+\left[\frac{\delta(s+1)}{2}\right]^{3} (J_{0}(z))^{2} \sum_{n>0} \frac{8J_{2n-1}(z)}{((2n-1)\Delta)^{2}} \sin(2n-1)\phi F_{y}$$

$$-\left[\frac{\delta(s+1)}{2}\right]^{3} J_{0}(z) \sum_{n\neq m\neq 0} \frac{4J_{n}(z)J_{m}(z)}{\Delta^{2}} \left\{ \frac{\cos n\phi \cos m\phi}{nm} F_{x} + \frac{m\cos n\phi \sin m\phi - n\sin n\phi \cos m\phi}{nm(m-n)} F_{y} \right\}.$$
(S27)

For s = 1 this becomes

$$H^{(3)} = \delta^3 \sum_{n>0} \left\{ \frac{4(J_{2n}(z))^3}{(2n\Delta)^2} \cos 2n\phi F_x - \frac{4(J_{2n-1}(z))^3}{((2n-1)\Delta)^2} \sin(2n-1)\phi F_y \right\} \approx \frac{\delta^3}{\Omega^2} \left(0.06 \cos 2\phi F_x - 0.4 \sin \phi F_y \right). \tag{S28}$$

Where we have used the fact that around the protection condition the sum is well approximated by the first term. Since for s = 1 the energy gap from Eq. (S19) is vanishing, both terms (F_x and F_y) contribute to the noise. The correction to the transition frequency due to inhomogeneous shift thus varies between

$$\Delta\omega_{\delta} \in (0.06, 0.4) \cdot \frac{\delta^3}{\Omega^2},\tag{S29}$$

depending on the phase ϕ . The lower noise amplitude is obtained when the two tones of the dressing are in-phase $\phi = 0$. For $s \gg 1$, the third-order Magnus term becomes

$$H^{(3)} \approx \frac{\delta^3}{\Omega^2} \left[-s(2 + \cos 2\phi) F_x + \sqrt{2} \sin \phi s^{3/2} F_y \right], \tag{S30}$$

which should be added to the second-order Magnus term [Eq. (S25)]

$$H_{\text{eff}}^{(2)} + H^{(3)} \approx \frac{\delta^3}{\Omega^2} \left(-sF_x + \sqrt{2}\sin\phi s^{3/2}F_y \right).$$
 (S31)

Once again, due to the large energy gap in the F_x direction, the perpendicular term ($\propto F_y$) produces a negligible perturbation. Therefore when $s \gg 1$, the first non-vanishing order correction to the transition frequency due to the inhomogeneous shift is

$$\Delta\omega_{\delta} \approx \frac{s\delta^3}{\Omega^2}.$$
 (S32)

A summary of these leading terms is presented in Table S1 (middle section).

S-.3. Protection by a dressing field with a stepwise-modulated phase

In our experiment, we did not explicitly employ the two-tone (symmetrically detuned) dressing of Eq. (S7). Instead, we passed a single-tone, resonant ($\Delta=0$) field through an electro-optic modulator and alternated its phase stepwise between 0 and π with a half-period T/2. This forms a multi-tone signal with a vanishing carrier, dominant first-order side bands, and additional higher-order side bands. The power spectral density of this signal thus highly resembles the pure two-tone case discussed in the previous section. However, an exact solution may be obtained for this case. The Hamiltonian alternates between H_+ and H_- , where $H_\pm=H_0\pm\Omega\sigma_x$. In analogy with the phase ϕ of the two-tone dressing in the previous section, here we control the duration of the initial interval (relative to the qubit initialization time t=0). We can describe the unitary evolution over the first full period T with

$$U_T = e^{-iH_-[1-f(\phi)]T/2}e^{-iH_+T/2}e^{-iH_-f(\phi)T/2},$$
(S33)

where $f(\phi) = \cos^2(\pi/4 - \phi/2)$. For an evolution time t = nT, the evolution operator is $U(t) = (U_T)^n$. One can see that the stepwise dressing with period T corresponds to the two-tone dressing with detuning $\Delta = 2\pi/T$. To expand U_T in leading orders of the inhomogeneous shift δ and the drive noise δ_{Ω} , we define an effective Hamiltonian H_{eff} by $U_T = \exp(-iH_{eff}2\pi/\Delta)$, such that H_{eff} can be expanded in orders of δ . The first order reads

$$H^{(1)} = \delta \frac{s-1}{2} \mathbb{I} - \delta \frac{s+1}{2} \frac{\sin(\pi\Omega/\Delta)}{\pi\Omega/\Delta} \left\{ \cos\left[(\pi\Omega/\Delta) \sin\phi \right] \sigma_z - \sin\left[(\pi\Omega/\Delta) \sin\phi \right] \sigma_y \right\}. \tag{S34}$$

Therefore, for protection up to first order we require:

$$\operatorname{sinc}(\pi\Omega/\Delta) = \frac{s-1}{s+1},\tag{S35}$$

where $\mathrm{sin}(x) = \sin(x)/x$. The protected dressed state is the eigenstate of the operator $F_x = -\cos\left[(\pi\Omega/\Delta)\sin\phi\right]\sigma_z - \sin\left[(\pi\Omega/\Delta)\sin\phi\right]\sigma_y$ with the eigenvalue -1 [Analogous to Eq. (S19)]. For $s\gg 1$, the condition (S35) can be expanded to leading order,

$$1 - \frac{(\pi\Omega/\Delta)^2}{6} + O((\pi\Omega/\Delta)^4) = 1 - \frac{2}{s} + O(s^{-2}).$$
 (S36)

We thus arrive at the condition $(\Omega/\Delta)^2 = 12/\pi^2 s \approx 1/s$, in agreement with both the one-tone and two-tone dressings at the $s \gg 1$ limit.

S-.3(a). Higher-order noise contributions

We maintain the notations of parallel ($\propto F_x$) and perpendicular ($\propto F_y, F_z$) noise terms in the dressed-state basis, where now $F_y = \cos\left[(\pi\Omega/\Delta)\sin\phi\right]\sigma_y - \sin\left[(\pi\Omega/\Delta)\sin\phi\right]\sigma_z$ and $F_z = \sigma_x$. The cross term of the drive noise together with the inhomogeneous shift is

$$H_{\delta \cdot \delta_{\Omega}}^{(1)} = \frac{1}{\Omega} \left\{ \left(\cos(\pi \Omega / \Delta) - \operatorname{sinc}(\pi \Omega / \Delta) \right) F_x - \sin \phi \sin(\pi \Omega / \Delta) F_y \right\} \cdot \left[\frac{s+1}{2} \delta \delta_{\Omega} \right]$$
 (S37)

As in the two-tone case, the perpendicular contribution vanishes when $\phi \to 0$. For a general ϕ , we examine the limits s = 1 and $s \gg 1$:

 \bullet For s = 1, under the protection condition (S35), the perpendicular term vanishes and we are left with the parallel term

$$\Delta\omega_{\delta\cdot\delta_{\Omega}} = \frac{\delta\delta_{\Omega}}{\Omega}. \tag{S38}$$

• For $s \gg 1$, this perpendicular term gives rise to a higher-order perturbation when the energy gap $\delta(s+1)$ [Eq. (S34)] is large enough. The leading contribution in the parallel term is:

$$\Delta\omega_{\delta\cdot\delta_{\Omega}} = 2\frac{\delta\delta_{\Omega}}{\Omega}.\tag{S39}$$

To second order in δ , the effective Hamiltonian reads

$$H^{(2)} = \frac{1}{\Omega} \operatorname{sinc} \left(\pi \Omega / \Delta \right) \left(\cos \pi \Omega / \Delta - \cos \left[(\pi \Omega / \Delta) \sin \phi \right] \right) \cdot \left(\frac{s+1}{2} \delta \right)^2 F_z. \tag{S40}$$

As in the two-tone case, the second-order contribution vanishes for $\phi \to \pi/2$ or for s = 1. For $s \gg 1$, we are left with $H^{(2)} \approx -\cos^2\phi(3/2)(\delta^2/\Omega)F_z$, which is perpendicular to the dressed state basis and thus only contributes a third-order correction

$$H^{(2)} \approx \cos^4 \phi \frac{9s}{4\Omega^2} \delta^3 F_x, \tag{S41}$$

assuming a large enough energy gap $\delta(s+1)$. For a general ϕ and s, the second-order term does not vanish. The effective Hamiltonian to the third order, for s=1, is $H^{(3)}=-\delta^3/(2\Omega^2)F_x$. For $s\gg 1$ the third order term is

$$H^{(3)} = -3s \frac{64 + 120\cos^4\phi}{160\Omega^2} \delta^3 F_x \tag{S42}$$

and, together with the higher order contribution of $H^{(2)}$, we obtain $H^{(2)} + H^{(3)} \approx -\frac{6s}{5\Omega^2} \delta^3 F_x$. the first non-vanishing order correction to the transition frequency due to the inhomogeneous shift is thus

$$\Delta\omega_{\delta} = \frac{6s}{5\Omega^2}\delta^3\tag{S43}$$

A summary of these leading terms is presented in Table S1 (right section).